



# Enhancing the vegetable waxes gelation power in the presence of high-intensity ultrasound

Thais Lomonaco Teodoro da Silva<sup>a,b,\*</sup>, Vincent Baeten<sup>c</sup>, Sabine Danthine<sup>a</sup>

<sup>a</sup> *Science des Aliments et Formulation, Gembloux Agro-Bio Tech, ULiège, 5030 Gembloux, Belgium*

<sup>b</sup> *Department of Food Science, Federal University of Lavras—UFLA, Lavras, Brazil*

<sup>c</sup> *Quality and Authentication of Products Unit, Quality Department of Agricultural Products, Walloon Agricultural Research Centre (CRA-W), Chaussée de Namur 24, 5030 Gembloux, Belgium*

## ARTICLE INFO

### Keywords:

Waxes  
Oleogels  
High-intensity ultrasound  
Minimum concentration for gelation

## ABSTRACT

The structuration of oils offers a promising alternative to high-saturated fats, capturing significant interest and undergoing development for two decades. Integrating high-intensity ultrasound (HIU) with oil structuration presents a compelling approach, as HIU has demonstrated its ability to alter numerous physical properties of fats with low saturated content. The primary aim of this study was to assess the impact of HIU on beeswax (BEW), candelilla wax (CLW), carnauba wax (CBW), and rice bran wax (RBW) oleogels. The minimum concentration required for oleogel formation (Cg) was established as the concentration at which the gel could maintain its structure without flowing when inverted. All oleogels in their Cg underwent sonication using a 13 mm probe, 50 % amplitude for 10s. The oleogels, whether sonicated or not, were evaluated based on their microstructure, hardness, viscoelastic properties, oil binding capacity (OBC), melting behavior, mild-infrared analysis, and X-ray. The amount of wax used to form a gel was quite low, especially for BEW (1.7 %) and CLW (1.4 %). After sonication, BEW, CLW, and CRW waxes significantly improved, mostly physical properties evaluated. On the contrary, RBW showed a depletory effect of physical properties after sonication in the condition tested. It was possible to observe that when appropriately optimized, sonication serves as a vital technique in the oleogelation of some waxes, offering a robust method to produce enhanced and stable oleogels suitable for food applications.

## 1. Introduction

Natural waxes have extensively been studied as oleogelators to form oleogels (Dassanayake et al., 2009; H.-S. Hwang et al., 2012; Patel et al., 2015; Toro-Vazquez et al., 2007). The significant interest in natural plant waxes stems from their high structuration power (1–5 %) (Patel et al., 2015), widespread availability, low cost, and thermoreversible properties (Doan, Tavernier, et al., 2017). Additionally, these waxes can function both as oleogelators and emulsifiers in emulsions, even without adding extra emulsifiers (Penagos et al., 2023), and they are mostly considered GRAS or approved by the FDA as food additives (Mattice & Marangoni, 2018).

Waxes are primarily composed of hydrocarbons, wax esters, long-chain fatty acids and alcohols, and triterpenoids, among other components. The proportion of each component varies significantly depending on the source, and the specific types of components present determine the final properties of the oleogel (Doan, To, et al., 2017).

Several waxes have been evaluated over the years as candelilla wax (CLW) (Toro-Vazquez et al., 2007), carnauba wax (CRW) (Blake & Marangoni, 2015), sunflower wax (SFW) (H.-S. Hwang et al., 2012), beeswax (BEW) (Martini et al., 2015), sugarcane wax (Rocha et al., 2013), shellac wax (Patel et al., 2013), berry wax (Doan, Tavernier, et al., 2017), fruit wax (Okuro et al., 2018), tea leaf wax, rapeseed wax, rose wax, and orange peel wax (Yilmaz, Keskin Uslu, & Öz, 2021), among others.

The most extensively used waxes for the formulation of oleogels and food applications are RBW, CLW, CRW, BEW, and SFW. Usually, waxes are classified as low molecular weight oleogelators, and when dispersed in the oil phase by direct dispersion and subsequently cooled, they form a crystal network that entraps the liquid oil, creating the gel structure (Patel & Dewettinck, 2015; Podmaniczky & Gránásky, 2022). This crystalline structure is associated with the classic phenomena of crystallization, divided into nucleation, growth, and stability of the crystalline network (Podmaniczky & Gránásky, 2022).

\* Corresponding author at: Department of Food Science, Federal University of Lavras—UFLA, Lavras, Brazil  
E-mail address: [thaissilva@ufla.br](mailto:thaissilva@ufla.br) (T.L.T. da Silva).

High-intensity ultrasound (HIU) has recently gained popularity as a supplementary method for altering the crystallization behavior of edible fats. HIU can customize the functional properties of lipids by promoting crystallization, decreasing crystal sizes, reducing oil migration, and phase separation, and creating firmer and more elastic crystalline structures (Chen et al., 2013; da Silva et al., 2020; Martini et al., 2008; Suzuki et al., 2010; Ueno et al., 2003; Ye & Martini, 2015).

HIU emits acoustic waves, and these waves have an impact on the crystallization that is known as sonocrystallization. The effect on fat crystallization steps has also been observed on oleogels (da Silva & Danthine, 2021; A. Giacomozzi et al., 2020; Rumayor-Escobar et al., 2023). HIU through cavitation changes the interactions between the oleogelator and oil and provides some specific benefits for oleogels as improving solubility of the oleogelator (Jadhav et al., 2022), reducing phase separation (Jana & Martini, 2014), improving synergism in multicomponent oleogels (da Silva & Danthine, 2021), reducing amount of oleogelator needed (A. Giacomozzi et al., 2020), and improving physical properties (Sharifi et al., 2019; Teodoro da Silva & Danthine, 2022).

Although many studies and benefits of using waxes to form oleogels have been reported to fully replace saturated fats, wax oleogels have still some challenges, such as sensory (Airoldi et al., 2022; da Silva et al., 2018), shear sensitivity (H. S. Hwang et al., 2013), limited aeration (da Silva et al., 2021), among others. Moreover, although waxes in general have shown a good structuration power, food applications have not been possible yet using waxes at their small critical gelling concentration. Thus, this study aims to apply HIU in different waxes-oleogels using the critical gelling concentration of beeswax (BEW), candelilla wax (CLW), carnauba wax (CRW), and rice bran wax (RBW) and verify the effect of HIU on improving crystallization and oleogel properties of each wax.

## 2. Material and methods

### 2.1. Material

Rapeseed oil was acquired from Royale Lacroix (Belgium), and its triacylglycerols composition is 29.3 % triolein (OOO), 22.6 % dioleoyl-linoleoyl glycerol (OOL), 12.1 % dioleoyl-linolenoyl (OOLn), and 6.5 % dioleoyl-palmitate glycerol (POO). Four waxes from Arome-Zone (Belgium) were used, beeswax (BEW), candelilla wax (CLW), carnauba wax (CRW), and rice bran wax (RBW).

### 2.2. Sample preparation

Oleogels (50 mL) were prepared by direct dispersion by heating the rapeseed oil with different types and concentrations of waxes at 90 °C/5 min in a 100 mL beaker over a heat plate using a 300 rpm magnetic stirring. The melted blend was then transferred to a water-cooled crystallization cell that was set close to the induction temperature of each wax (Table 1). The system was then cooled under magnetic stirring (150 rpm) until the first crystals appeared at the  $T_c$  of each wax (Table 1). After the first crystals were visualized, the sample (50 mL) was either collected without HIU (wo HIU) or sonicated (with HIU). Sonication was done using a 13 mm probe for 50 % amplitude ( $53 \pm 2$  W) and 10s in a crystallization cell of 100 mL. HIU used a 20 kHz CPX 750, Cole 115 PA Parmer Instruments (Illinois, USA). After sonication, samples were also placed in 100 mL plastic containers (filling 2.5 cm of the container) and stored in an incubator at  $20 \pm 0.5$  °C for the second static cooling step ( $\sim 0.5$  °C/min) and stored for 24 h before further analysis. Oleogels with or without HIU were prepared in triplicate.

**Table 1**

High Intensity Ultrasound (HIU) and oleogelation process and characteristics of each wax and wax-oleogel in this study.\*

Crystallization/HIU conditions	Waxes			
	BEW	CLW	CRW	RBW
Wax MP (°C)	68.5 ± 0.1	72.1 ± 0.1	82.4 ± 0.1	78.6 ± 0.1
Cg (%)	1.7	1.4	4.2	6.0
$T_{G'=G''}$ (°C)	40.0 ± 0.6 <sup>c</sup>	38.3 ± 0.6 <sup>c</sup>	49.8 ± 2.8 <sup>b</sup>	58.3 ± 0.2 <sup>a</sup>
$T_c$ (°C)*	42.9 ± 1.0	35.2 ± 1.0	62.2 ± 1.0	60.7 ± 1.0
Induction time (min)	4 min	4 min	1.75 min	2.0 min
HIU conditions				
Power (W)	53 ± 2.0	53 ± 2.0	53 ± 2.0	53 ± 2.0
Duration (s)	10	10	10	10

\* Cg: critical gelling concentration,  $T_c$ : Temperature of the first crystals,  $T_{G'=G''}$ : cross over temperature, MP: melting point, BEW: bees wax, CLW: candelilla wax, CRW: carnauba wax, RBW: rice bean wax.

## 3. Methods

### 3.1.1. Critical gelling concentration

The critical gelling concentration (Cg) was evaluated for the four waxes by using two techniques. Samples without any sonication were prepared using several concentrations with 0.2 g variation on 20 mL plastic containers. After the 24 h stabilization at 20 °C, the containers were turned upside down and kept for 10 min as shown in Fig. 1, to identify the concentration ranges where the gels did not flow under the influence of gravity. The critical gelling concentration was the smallest concentration where a self-sustainable gel was formed and no flow was observed. To confirm the gel formation, samples close to the visual Cg were evaluated using rheological characterization with a modular compact rheometer MCR 302 (Rheoplus, Anton Paar, Austria). An oscillatory frequency sweep at a constant stress of 0.02 Pa was performed, and the resultant values of elastic and viscous modulus ( $G'$  and  $G''$ , respectively) were compared at low frequency. The corresponding concentrations at which  $G' > G''$  were identified as Cg for individual waxes (Patel et al., 2015).

### 3.1.2. Microstructure

The wax oleogel microstructure was evaluated using polarized-light microscopy (PLM, Nikon Eclipse E400, Kanagawa, Japan). The images were obtained with the digital camera (Nikon, DS-Fi2, Tokyo, Japan) coupled to the microscopy. Microstructure was evaluated using a 20× magnification objective after a drop of the crystallized oleogel was placed between a slide and a cover slide. The crystal diameter mean was measured for each sample, and 12 images of the three different replications were captured using a 20× objective. Image analysis was performed using the software Image Pro-Plus (Media Cybernetics, Rockville, MD, USA).

### 3.1.3. Melting behavior

The melting behavior and melting point of the oleogels and waxes were assessed using differential scanning calorimetry (DSC), Q2000 DSC (TA Instruments, New Castle, DE, USA). DSC was calibrated using indium and eicosane and coupled with a refrigeration cooling system (TA Instruments, New Castle, DE, USA). Eight to twelve milligrams of oleogel or pure wax were weighed in the T-zero hermetic pan, and an empty pan was used as a reference. For waxes melting point the samples were first heated to 100 °C using a 5 °C/min heating rate and kept at 100 °C for 15 min to guarantee complete melting; after this, they were crystallized using a 5 °C/min cooling rate until  $-20$  °C and kept at this temperature



**Fig. 1.** Minimum concentration of waxes necessary to visually self-structure the oleogel. Carnauba wax example, from left to right, 4.0, 4.2 and 4.4 % (w/w) of wax in rapeseed oil.

for 90 min. The last step was a second melting to 100 at 5 °C/min heating rate. The peak temperature ( $T_p$ ) obtained from the last melting step was used to quantify the melting point. The melting behavior of the oleogels in their Cg with or without HIU was also evaluated using a DSC. For this analysis, the oleogels were stabilized at 20 °C for 1 min and then heated to 100 °C using a 5 °C/min heating rate. The melting curves were recorded using the Universal Analysis Software version 4.2 (TA Instruments, New Castle, DE, USA). The parameters assessed were onset temperature ( $T_{on}$ ), peak temperature ( $T_p$ ), end temperature ( $T_{end}$ ), and enthalpy ( $\Delta H$ ).

### 3.1.4. Rheology

The rheological behavior of the oleogels with or without HIU was measured using a modular compact rheometer MCR 302 (Rheoplus, Anton Paar, Graz, Austria). The geometry of 1° cone plate of 40 mm diameter and 102 μm gap was used for all measurements. (a) Viscosity was measured using a structured recovery (thixotropy) condition, and three-sequence intervals were measured: (1) 2 min shear rate at 0.1 s<sup>-1</sup>, (2) 2 min shear rate at 1.0 s<sup>-1</sup>, and (3) 2 min shear rate at 0.1 s<sup>-1</sup>. The average of the first curve was used as the viscosity (Pa.s) of the sample. Afterward by comparing the first and third curves the structure recovered (%) was also evaluated. (b) Strain sweeps were evaluated from 0.0008 to 100 % strain at 1 Hz. The results of viscoelasticity ( $G'$  and  $G''$ ) were calculated as an average of the linear viscoelastic region (LVR) using the Rheoplus software (Anton Paar, Austria). (c) The frequency sweeps were evaluated by varying the angular frequency from 0.1 to 100 rad/s, with a fixed LVR amplitude of  $\tau = 0.01$  Pa. (d) A temperature ramp was also performed with an oscillatory stress of 0.02 Pa, frequency = 1 Hz, and temperature variation from 90 to 20 °C, at a 2 °C/min cooling rate. The temperature where  $G' = G''$  was used to correlate with the  $T_c$  to confirm the induction time to apply HIU. All samples were analyzed in quadruplicate for each test.

### 3.1.5. X-ray diffraction

Polymorphism of the oleogels was evaluated by X-ray diffraction, using a Bruker D8 Advance Diffractometer (Bruker, Germany). A LynxEye detector (Bruker, Germany), with Cu K radiation (= 1.54178 Å, 40 kV, 30 mA) was used. The short and long spacing were evaluated (1 to

27°). The step size of the measurements was 0.02°. To improve peak visualization samples were filtered before analysis.

### 3.1.6. Oil loss

The non-entrapped oil in the oleogel network was evaluated by centrifugation according to da Silva and Danthine (2021). A 5810R Eppendorf centrifuge was used, for 15 min at 10000 rpm. Approximately 1 g of stabilized oleogel was used. An empty Eppendorf ( $w_a$ ), an Eppendorf with oleogel ( $w_b$ ), and the Eppendorf after oil linking ( $w_c$ ) were weighted. Calculation of the oil loss was done following eq. 1. Analysis was performed in quadruplicate.

$$\text{Oil loss} = \left( \frac{w_c - w_a}{w_b - w_a} \right) * 100 \quad (1)$$

### 3.1.7. MIR analysis

The ATR-FT-MIR spectra of oleogels were acquired using a Bruker Vertex 70 Fourier transform spectrometer equipped with an ATR golden gate accessory. The spectra were acquired (4000–600 cm<sup>-1</sup>) with a resolution of 4 cm<sup>-1</sup> with 64 co-added scans. The spectral acquisition was done using OPUS 6.5 (Bruker) software. The reference spectrum used was the air spectrum collected before each sample analysis. The analysis was done in triplicate.

## 3.2. Statistics

Each process and analytical measurement were performed in replicates as described above. The results were submitted to analysis of variance (ANOVA) using Minitab 18 software. Means were compared using Tukey's test with a significance level of 5 % ( $\alpha \leq 0.05$ ).

## 4. Results and discussion

### 4.1. Critical gelling concentration (Cg)

Each wax has shown a different Cg after tube flipping that was confirmed by rheological measurements (where  $G'$  was higher than  $G''$  at a low shear rate) as shown in Table 1. The higher structuration power was shown by CLW and the lower one by RBW. Similar values and order

have been found previously, with slight value changes due to storage temperature (Doan et al., 2015; H.-S. Hwang et al., 2012; Patel et al., 2015; Shi et al., 2021). The different  $C_g$  of the different waxes have been attributed to the solubility of the wax in the solvent (Co & Marangoni, 2012), and the different chemical compositions of them (Doan, To, C. M., et al., 2017).

The ability of the wax to form an oleogel is believed to be a balance between the solubility and insolubility of the oleogelator within the solvent, an oleogelator molecule must be relatively insoluble so that it can crystallize or self-assemble to form mesoscale structures. Yet, the oleogelator must be relatively soluble such that it can interact with solvent molecules (Co & Marangoni, 2012).

Regarding the composition, waxes composition used has been previously described (Doan, Tavernier, et al., 2017). BEW is composed of a mixture of wax esters (58.0 %), hydrocarbons (26.9 %), free fatty acids (8.8 %), and free fatty alcohols (6.4 %). The CLW is major composed of hydrocarbons (72.9 %), with small amounts of wax esters (15.8 %), free fatty acids (9.5 %), and free fatty alcohol (2.2 %). CRW as BEW has a higher concentration of wax esters (62.0 %), a representative amount of free fatty alcohols (30.7 %), and free fatty acids in small amounts (6.8 %). RBW is the purer of the waxes in this study with 93.7 % of wax ester and only 6 % of free fatty acids (Doan, To, C. M., et al., 2017). These compositions suggest that the  $C_g$  is affected not only by the type of single component (wax ester, or hydrocarbons) but also by the combination of them, the carbon chain size, and the presence of minor components like free fatty acids and fatty alcohols and their types. Hwang et al. (2012) affirmed that reliable gelling abilities were evident with several wax minor components as (a) wax esters than with p-hydroxycinnamic aliphatic di-ester, (b) saturated alkyl chains of esters, (c) longer alkyl chains of wax esters, and (d) wax esters.

The following concentrations were further evaluated with and without HIU: BEW 1.7 %, CLW 1.4 %, CRW 4.2 %, and RBW 6.0 % considering their  $C_g$ . These findings indicate that waxes are highly effective structuring agents, as only a minimal amount of wax is required to structure large quantities of oil (Blake et al., 2014).

## 4.2. Rheology

### 4.2.1. Temperature sweeps

Temperature sweep curves can be found in Fig. S1 and the temperatures where  $G' = G''$ , or cross-over temperature ( $T_{G'=G''}$ ) are presented in Table 1. Except for CRW all waxes  $T_{G'=G''}$  were very close to the visual  $T_c$ , confirming the HIU was applied in the presence of small amounts of crystals.

Higher  $T_{G'=G''}$  was observed for RBW, followed by CRW and BEW and CLW showed similar values ( $p > 0.05$ ), similar to those previously observed by (Patel et al., 2015).

CRW and RBW have a higher amount of oleogelator (4.2 and 6.0 % respectively) and showed a  $G' > G''$  faster than CLW and BEW, suggesting that their crystallization is followed by a great extensive microstructure development (Patel et al., 2015).

### 4.2.2. Amplitude sweeps

Amplitude sweeps are shown in Fig. 2A, all oleogels showed  $G' > G''$  with or without HIU, confirming their gel formation and behavior even in higher shear rates. For viscoelastic materials, the frequency-dependent functions  $G'$  and  $G''$  give a measure of solid-like and liquid-like characteristics, respectively. Typically, for gels the elastic component ( $G'$ ) dominates over the viscous component ( $G''$ ) at small applied shear and attains a plateau in the linear response region (LVR, or linear viscoelastic region) (Menard & Menard, 2020). Comparing the 4 evaluated waxes, RBW showed higher viscoelasticity, while CRW, CLW, and BEW showed similar viscoelasticity ( $p > 0.05$ ).

HIU significantly improved the  $G'$  and  $G''$  of the BEW, CLW, and CRW oleogels ( $p < 0.05$ ). A similar result was observed for 3 % CLW-oleogel on several nut oils (Li et al., 2021), and 8 % CRW-oleogel (Sejwar et al.,

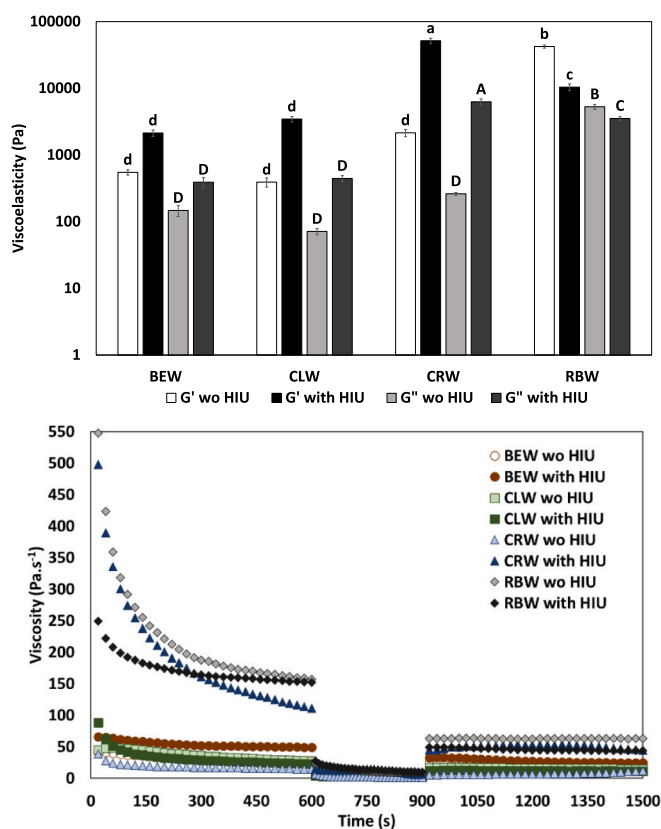


Fig. 2. (A) Viscoelasticity of the wax oleogels with and without HIU was obtained in the linear viscoelastic region by amplitude sweeps. Samples followed by the same letter, upper ( $G'$ ) or lower ( $G''$ ) case, are similar to each other ( $\alpha = 0.05$ ). (B) Thixotropic recovery measurements of the waxes oleogels with and without HIU.

2024), suggesting that sonication has a significant role in strengthening the oleogel structure of some waxes.

Nevertheless, surprisingly the viscoelasticity of the RBW was significantly reduced after sonication ( $p < 0.05$ ). HIU in monoglycerides-oleogels has also shown a reduction in viscoelasticity compared to the non-sonicated sample (da Silva & Danthine, 2021). In the case of monoglycerides, it was found that the moment where HIU was applied is very important in very high-melting point samples. When not optimized instead of inducing crystallization of the oleogelator, HIU can retard this process resulting in a weaker structuration of the oil (da Silva & Danthine, 2021; A. Giacomozzi et al., 2020).

### 4.2.3. Thixotropy

Thixotropy curves are presented in Fig. 2B, the viscosity and recovery stats can be found in Table S1. Oleogels formed by BEW, CLW, and CRW all showed an improvement in viscosity after sonication (BEW 30.8 to 50.6 Pa.s<sup>-1</sup>, CLW 33.3 to 37.2 Pa.s<sup>-1</sup>). However, only CRW showed a significant increase from 22.8 to 211.1 Pa.s<sup>-1</sup> due to sonication ( $p < 0.05$ ).

RBW as for other amplitude sweeps also showed a significant reduction in viscosity after HIU application (232.3 Pa.s<sup>-1</sup> with HIU, and 169.5 Pa.s<sup>-1</sup> with HIU).

Among all wax oleogels the better recovery properties were 60.4 % for BEW. CLW and CRW showed similar recovery properties (~40 %) and RBW had very low recovery power (33.9 %). Patel et al. (2015) also found higher recovery properties for the BEW, however in their work a lower recovery was observed by the CRW gel. The authors attributed this to the agglomerated crystals formed for CRW, which upon enough shear to start the flow, deagglomerate and lose their structure. BEW, on another hand, although showing an easy initiate flow, might correspond

to a weaker but uniform type of bonding (homogeneous bonding strength), resulting in a flow-induced structure breakdown that is non-time-dependent (Patel et al., 2015). Results that might be corroborated also with the CLW-oleogel, and RBW-oleogel.

Besides viscosity and recovery, a different behavior for CRW could be observed. At the first step of the curve a very high viscosity is observed in a short time, however, compared to the others, CRW-oleogel showed a very fast decline in viscosity values. This suggests that a very high force is required to initiate the flow compared to maintaining the flow, this confirms the loss of structure upon shear as proposed by Patel et al. (2015).

All sonicated samples showed a lower recovery than their corresponding non-sonicated ones ( $p < 0.05$ ), except for the RBW sample. RBW sample showed a similar recovery ( $p > 0.05$ ) among sonicated a non-sonicated sample, and the lowest recovery among all oleogels. Sonication usually induces the structuration of the tridimensional network by cavitation and improves the physical properties of viscoelasticity. All samples showed an improvement in viscosity after sonication which suggests that HIU has been acting on the wax structuring effect. After shearing, all samples showed the same viscosity (with or without HIU). Thus, we believe that either (1) the high shear is inhibiting the sonication effect, or (2) the recovery is lower simply because the initial viscosity is higher.

#### 4.2.4. Frequency sweeps

Frequency sweeps are shown in Fig. 3. The frequency sweeps were conducted to investigate the time-dependent deformation behavior. Within the angular frequency range of 0.1 to 100 rad/s, the  $G'$  and  $G''$  curves were predominantly linear, with  $G'$  exceeding  $G''$ , especially for BEW and CLW samples. This indicates that the gels exhibited good tolerance to the rate of deformation and that the bonds forming the network were almost permanent within the timeframe of the test (Daniel & Rajasekharan, 2003).

All the samples displayed a slight frequency dependence over 100 rad/s, characteristic of a weak gel, as evidenced by a slightly positive slope in the  $G'$ . This is typical behavior of a weak colloidal gel, where the viscoelastic properties are dominated by viscosity at low frequencies and

by elasticity at high frequencies (Trappe & Weitz, 2000). Once the elastic modulus  $G'$  is plotted as a function of frequency, strong gels show a constant value (frequency independence) while weaker gels display frequency-dependent behavior and will have an increasing  $G'$  as a function of the frequency (Tavernier et al., 2018).

Sonication showed a lower effect on the frequency sweeps than other rheology parameters at lower frequencies (100 rad/s), suggesting that HIU does not change the frequency dependency of oleogels at the Cg. Nonetheless, at higher frequencies ( $>100$  rad/s) it seems that after sonication there is a more linear behavior, suggesting the formation of a stronger gel (Tavernier et al., 2018).

#### 4.3. Microscopy

In natural waxes, the crystal morphology and crystalline structure are determined by the chemical composition, polarity, chain length, and melting point of the dominant components (Abdallah & Weiss, 2000). Crystal morphology of the oleogels can be found in Fig. 4.

BEW oleogel was formed by small needle-like crystals (diameter mean [Dm] of  $3.16 \pm 0.11 \mu\text{m}$ ) well organized and distributed confirming previous studies (Shi et al., 2021). The formation of needle-like crystals was driven by the interaction of Van der Waals forces between long-chain hydrocarbons and polar ester groups within the lamellar plane, leading to an increased rate of lateral growth (Dassanayake et al., 2009). Sonication has changed the BEW oleogel microstructure, reducing significantly the Dm to  $2.52 \pm 0.06 \mu\text{m}$  and increasing the number of crystals present. These crystals also seem to be more interconnected to each other which justified the improved rheological measurements observed. HIU was applied on this sample in the presence of primary crystallization, which suggests that cavitation, in this case, is either inducing secondary nucleation early, increasing the number of crystals at early stages of the nucleation and avoiding further crystal growth, or breaking up primary nucleus formed what also increases the number of the nucleus. This effect was also observed previously when HIU was applied at Tc for other types of oleogels (da Silva & Danthine, 2021; A. Giacomozzi et al., 2020) and it was attributed to cavitation. According to Leighton, sonication generates acoustic waves that travel

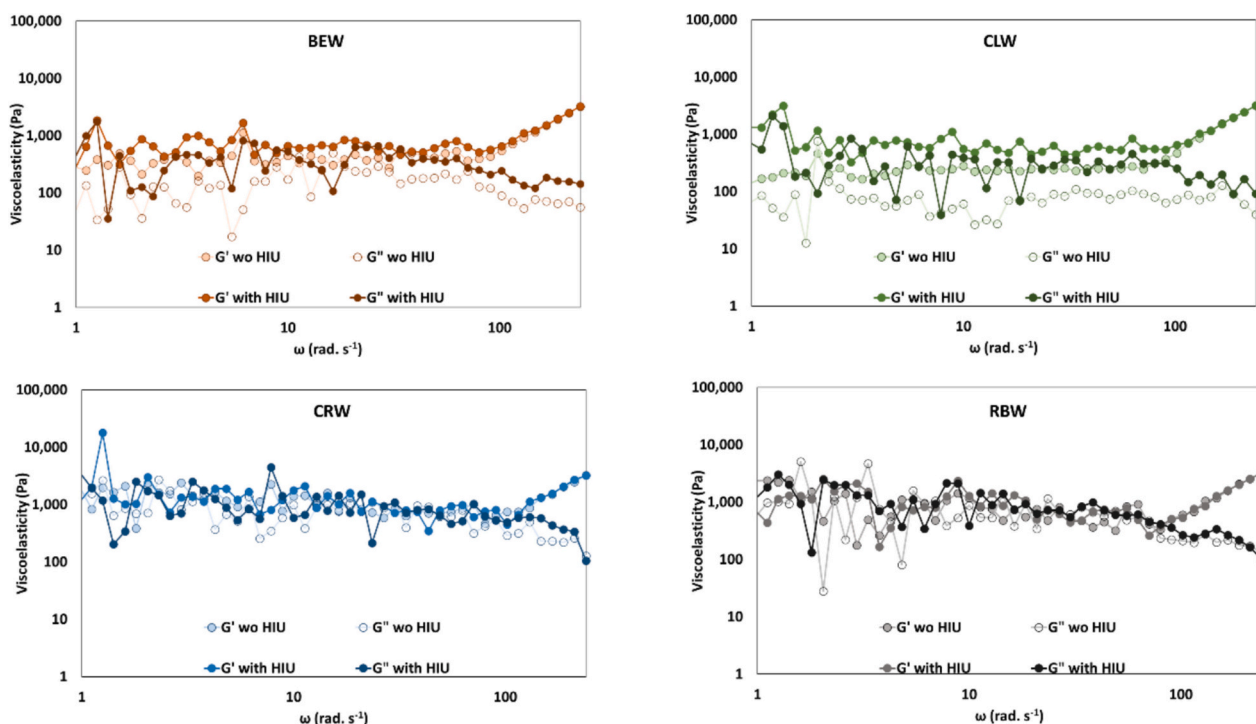


Fig. 3. Frequency sweeps for oleogels made at the Cg of respective waxes.  $G'$  and  $G''$  are shown as filled and open symbols, respectively.

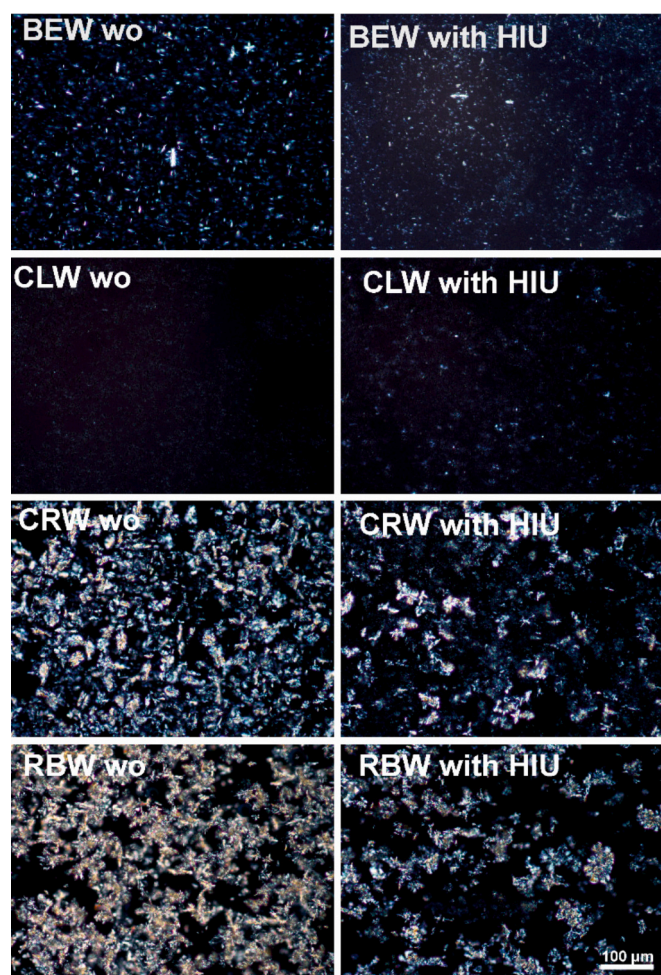


Fig. 4. Crystal morphology of wax-oleogels with and without High-Intensity ultrasound at  $C_g$  of each wax (BEW: bees wax; CLW: candelilla wax, CRW: carnauba wax, and RBW: rice bran wax). Images taken using a  $20\times$  objective, white bar represents  $100\ \mu\text{m}$ .

through a material generating the displacement of molecules around an equilibrium position. In the case of HIU, when the pressure of the acoustic wave reaches a specific threshold the zones of low pressure will generate a void, that transforms into a cavity or bubble. Through the interval of the sonication, these bubbles can oscillate around their equilibrium position, or they can grow and eventually collapse when enough acoustic power is applied. The formation and lifecycle of a bubble are called “cavitation”. When a specific power threshold intensity is reached, the bubble collapses. Bubble collapse is a very aggressive phenomenon and generates extreme and localized temperatures ( $5000\text{--}10,000\ \text{K}$ ) and high shear forces and pressures ( $100\text{--}5000\ \text{atm}$ ). These events are responsible for generating physicochemical changes in the material (Leighton, 1994). In crystals as observed by BEW-oleogel, this cavitation induces primary and secondary nucleation increasing the amount of crystals and reducing their size (Suzuki et al., 2010).

The CLW oleogel showed a microstructure based on microplatelets ( $D_m = 1.79 \pm 0.05\ \mu\text{m}$ ) as previously observed (da Silva et al., 2019, 2022; Patel et al., 2015). After sonication, the crystal size was significantly similar,  $D_m = 1.80 \pm 0.02$ . However, the number of crystals observed was a lot higher, suggesting that HIU might also improve the crystalline network of the CLW, and form a more organized and interconnected crystalline network. Both CLW and BEW needed a very small amount of wax ( $C_g$ ) to form a self-sustainable oleogel, this is interconnected with the type of crystal morphology and the presence of small crystals. Small

platelet crystals, in particular, tend to assemble easily and can hold a greater amount of oil due to their larger surface area, which enhances their ability to bind the oil (Blake et al., 2014; Patel et al., 2015).

CRW oleogel showed a crystalline network formed by crystal aggregates. Some needle-like structures ( $D_m = 4.38 \pm 0.27\ \mu\text{m}$ ) are seen in these agglomerates. The tendency to agglomerate and form heterogeneous structures is typically associated with a reduced structuring capability. Consequently, a moderately higher crystalline mass fraction of CRW was required for effective network formation (Patel et al., 2015). Sonication has also affected the crystalline network of the CRW gel, after HIU CRW oleogel showed fewer agglomerates, with smaller crystals ( $D_m = 3.81 \pm 0.10\ \mu\text{m}$ ) due to the cavitation.

RBW also was formed by small structures ( $3.94 \pm 0.24$ ) in agglomerates (non-sonicated sample). In our work, these small structures resemble needle-like crystals as reported by Doan et al. (2015), but depending on the solvent RBW seems to form a long fiber-like structure (Shi et al., 2021). After sonication the RBW oleogel showed visually less crystalline material and bigger agglomerates, although no significant difference was found in the crystal size ( $4.14 \pm 0.14\ \mu\text{m}$ ). Thus, in this case, instead of improving the oleogelator crystal network, HIU seems to break the structure even more. Monoglycerides-oleogels have shown the same behavior (da Silva & Danthine, 2021; A. S. Giacomozzi et al., 2019; Teodoro da Silva & Danthine, 2022). The different authors have found that the very fast crystallization of the high-melting-point monoglycerides makes it hard to apply HIU at the appropriate moment of the crystallization to induce crystallization, and instead, it retards it. RBW is the wax with a higher concentration of wax ester ( $\sim 93\%$ ), with a high melting point, and the wax that uses the higher  $C_g$ . Those factors combined might be the cause of the inefficiency of sonication in inducing the crystallization and improving the physical properties of this gel.

#### 4.4. Oil loss

The oil binding capacity of the oleogels with and without HIU can be observed in Fig. 5. The oil binding capacity (OBC) is another important indicator, expressing the strength and nature of gelator-solvent interaction, especially when the gel is mechanically stressed (Blake et al., 2014). Due to the small amount of wax used ( $C_g$ ), the oil leakage was quite high for all waxes ( $20\text{--}50\%$ ). CLW-oleogel was the one with lower oil loss, and CRW in contrast to the one with a higher amount of oil loss, a similar order ( $\text{CLW} < \text{RBW} < \text{CRW}$ ) has been previously found (Blake & Marangoni, 2015). Even though it has spherical morphology, the CRW-oleogel showed a higher OBC than the RBW-oleogel, which featured needle-like crystals. The extensive surface area and wide dispersion of CLW crystals throughout the oil phase enabled a greater quantity of liquid oil to be adsorbed and retained within the crystalline network (Blake & Marangoni, 2015). By contrast, the CRW and RBW crystals had less surface area and less homogeneous dispersion in the oil phase, explaining the easier release of liquid oil from the network or a lower OBC. The high OBC is attributed to the small size of wax particles (smaller void spaces making it difficult for oil to leak out) and also the uniform distribution of particles in the material (Blake et al., 2014).

Previously, it was found that in terms of oil loss, HIU parameters such as power level, and duration had significant effects (Sharifi et al., 2019). Conversely, although BEW and CLW oleogels showed improved rheology and higher crystal density after sonication, they showed a higher amount of oil loss on sonicated samples. It seems that a positive correlation between HIU and cooling rate is very important to have a positive effect on oil loss (A. S. Giacomozzi et al., 2019; Sharifi et al., 2019). Usually, a better improvement was found when a slow cooling rate was used (A. S. Giacomozzi et al., 2019).

CRW and RBW on another hand have shown a significant improvement in oil binding capacity after HIU has been applied ( $p < 0.05$ ). Crystal structure does not appear to account for the variations observed in phase separation based on the type of oil used; however, spherulites

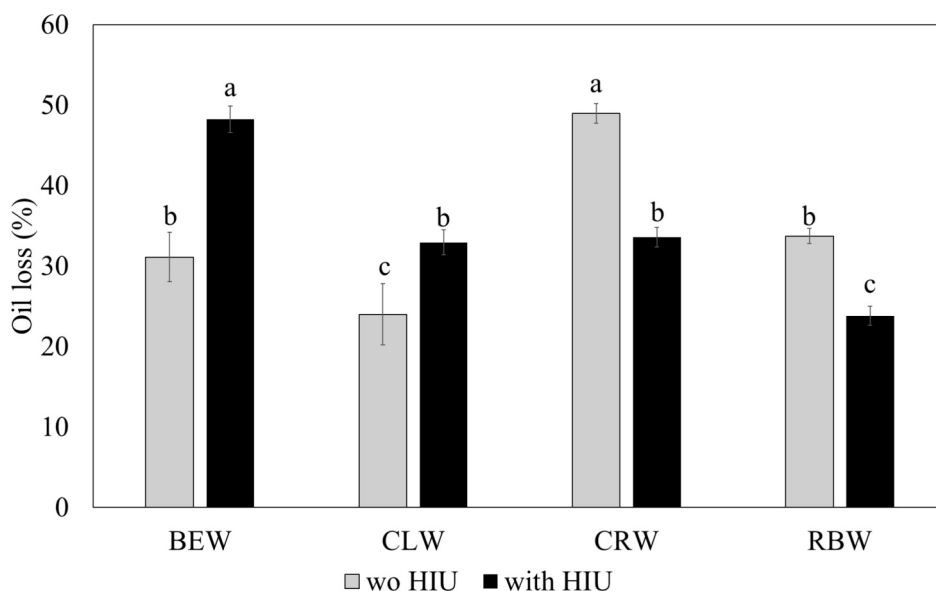


Fig. 5. Oil loss of the wax-oleogels with and without HIU. Samples followed by the same letter are similar to each other ( $\alpha = 0.05$ ).

seem to be more frequently linked with phase separation. Typically, HIU disrupts the spherulites, resulting in the formation of small needle-like crystals. It was projected that these needle-like crystals could work together easily with one another, leading to greater oil entrapment and by this means postponing phase separation (Jana & Martini, 2014).

#### 4.5. Melting behavior

Melting behavior curves are presented in Fig. 6, and the meeting data can be seen in Table S2. There is a significant difference between the different waxes, which is attributed to the difference in chemical composition (Doan, To, et al., 2017).

Although Sonication has shown a tendency to dislocate the peaks to a lower  $T_p$  (Fig. 6), there is no significant difference in this melting parameter at the same wax with or without HIU (Table S2). Da Silva et al. (2019) have also not found any significant change in the melting behavior of oleogels due to sonication.

Widespread melting profiles of sonicated samples exhibit a lower peak temperature and/or “shoulders” at lower temperatures, produce a crystalline matrix with a narrower melting peak, or increase the melting enthalpy of the system. Results that are also flowed by changes in microstructure, and amount of solid material formed (da Silva et al., 2020). Nevertheless, the changes in the micro and macrostructure of this work were not followed by any change in melting behavior, which can

be due to the very low amount of wax used.

#### 4.6. X-ray diffraction

The X-ray diffraction of the wax oleogels with or without HIU can be found in Fig. 7A. All waxes exhibited peaks only in the wide angle, and they all showed only peaks at 4.2 and 3.8 Å. Similar peaks have been previously found for wax-oil blends (Dassanayake et al., 2009; Sharifi et al., 2019; Shi et al., 2021).

HIU did not influence the crystalline structure, which suggests that HIU does not affect the polymorphic form. This is in agreement with previous work that showed that although HIU changed the morphology of the crystals, there was no change in the polymorphic form (da Silva & Danthine, 2021; Sharifi et al., 2019; Ye et al., 2011) The result suggested that HIU application could influence on crystallization of oleogels without changing the crystal form (Sharifi et al., 2019).

#### 4.7. MIR analysis

The MIR analysis provides information about the molecular interactions of oleogels. The gelation of oleogel mainly comes from hydrogen bonds or van der Waals force (Dassanayake et al., 2009). Curves obtained from the MIR analysis can be observed in Fig. 7B. The general peaks that symbolize triglyceride functional groups in oils and

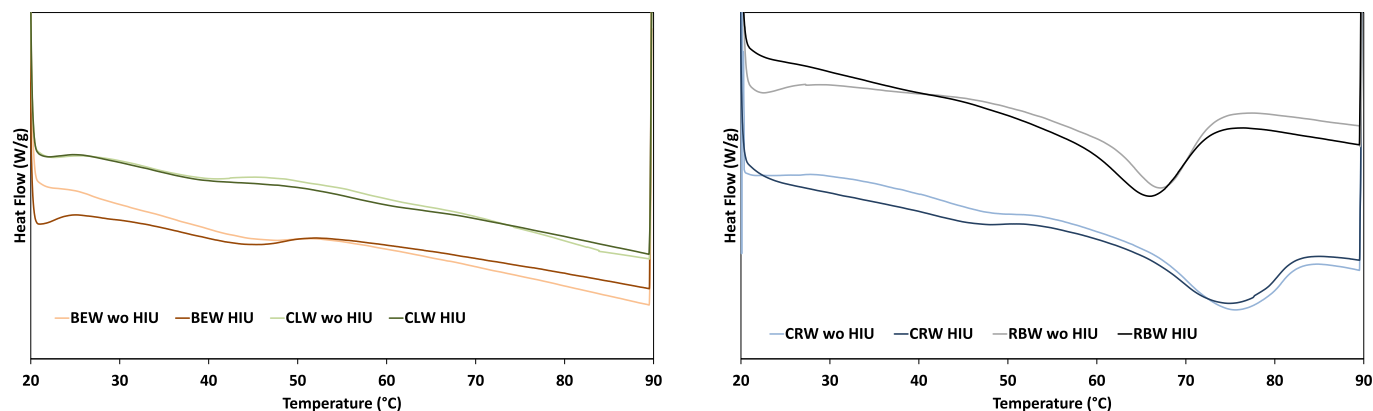


Fig. 6. Melting curves of the wax-oleogels with and without HIU.

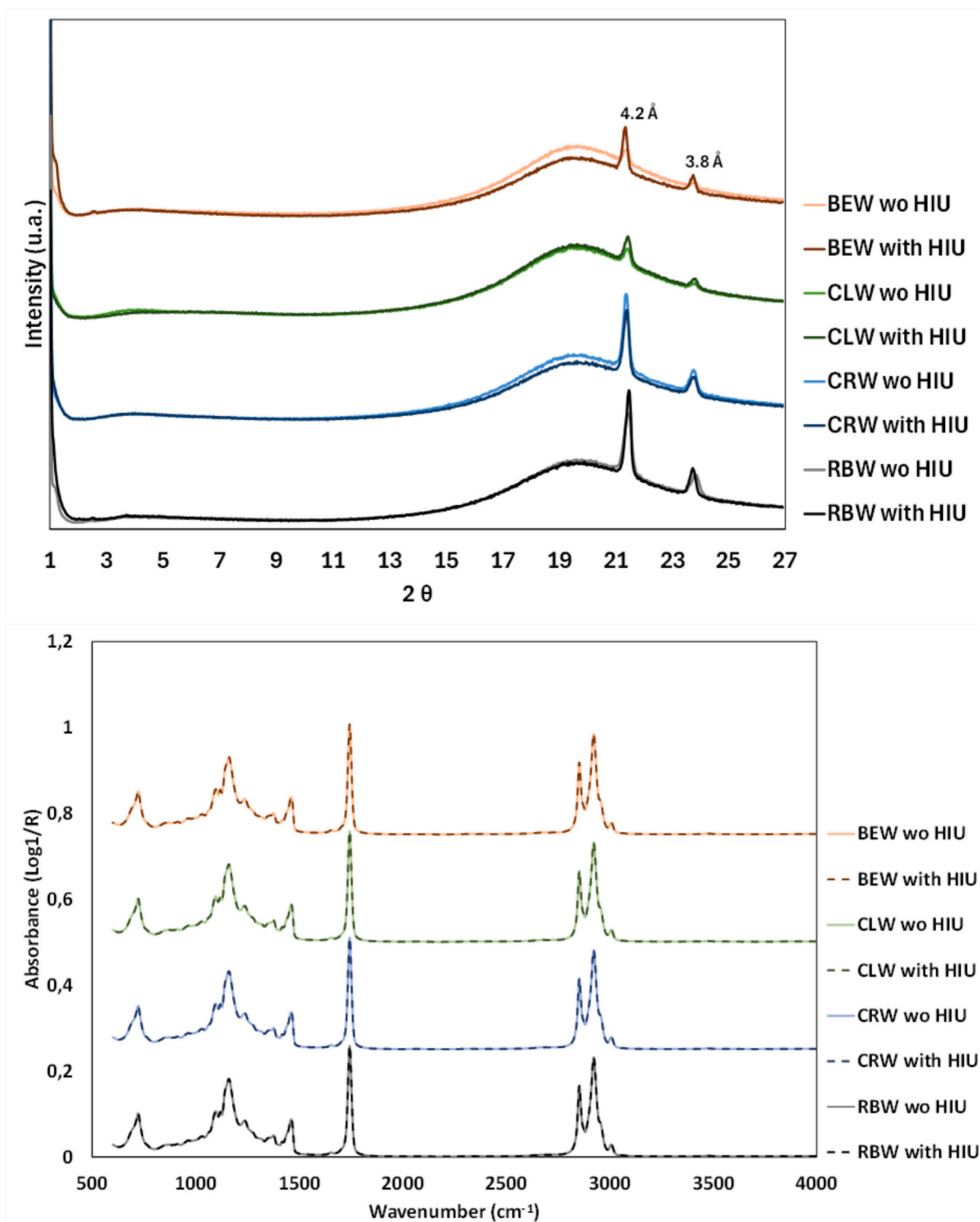


Fig. 7. X-ray diffraction (A) and FT-MIR spectra (B) of the wax-oleogels with and without HIU.

fats are observed around  $2937\text{ cm}^{-1}$  (C—H stretching (asymmetry)),  $2856\text{ cm}^{-1}$  (C—H stretching (symmetry)),  $1749\text{ cm}^{-1}$  (C—O stretching),  $1454\text{ cm}^{-1}$  (C—H bending (scissoring)),  $1166\text{ cm}^{-1}$  (C—O stretching and C—H bending), and  $709\text{ cm}^{-1}$  (C—H bending (rocking)) (Guillen & Cabo, 1997). All these bands were observed in this study, and as previously described are mostly from the rapeseed oil functional groups (da Silva et al., 2023). Sonication has induced no change in the chemical interactions of the wax with the oil.

## 5. Conclusion

It is possible to improve the physical properties of the waxes-oleogels even in their Cg, suggesting that is even possible to reduce the minimum amount of wax needed to form an oleogel.

BEW, CLW, and CRW gels are more easily induced by sonication, RBW on the hand, with the condition tested, did not benefit from HIU. HIU in BEW, CLW, and CRW improved the rheological properties, and those changes were followed by changes in the microstructure and

organization of the wax's crystals. Although the crystal size and distribution have changed, no changes were observed in the melting behavior, polymorphism, and chemical interactions after sonication of those oleogels.

Thinking about food application in lipid-based foods such as margarine and spreads, a physically improved oleogel with a lower amount of oleogelator is very important since it is cheaper and more technologically applicable, moreover would provide higher chances of sensory acceptance.

#### CRedit authorship contribution statement

**Thais Lomonaco Teodoro da Silva:** Writing – review & editing, Writing – original draft, Visualization, Validation, Resources, Project administration, Methodology, Investigation, Funding acquisition, Formal analysis, Data curation, Conceptualization. **Vincent Baeten:** Writing – review & editing, Methodology, Data curation. **Sabine Danthine:** Writing – review & editing, Supervision, Methodology.

#### Declaration of competing interest

The authors declare that they have no known competing financial interests or personal relationships that could have appeared to influence the work reported in this paper.

#### Acknowledgments

The authors are grateful for the Postdoctoral fellowships and funding in Sciences, Technology, Engineering, Materials, and Agrobiotechnology (STEMA) funding OTP N° DIVE.0899-J-P given by Liège, University Research Council. The authors also thank Quentin Arnould from CRA-W for the support in the MIR analysis.

#### Appendix A. Supplementary data

Supplementary data to this article can be found online at <https://doi.org/10.1016/j.foodchem.2025.143789>.

#### Data availability

Data will be made available on request.

#### References

- Abdallah, D. J., & Weiss, R. G. (2000). n-Alkanes gel n-alkanes (and many other organic liquids). *Langmuir*, 16(2), 352–355. <https://doi.org/10.1021/la990795r>
- Airoldi, R., da Silva, T. L. T., Ract, J. N. R., Foguel, A., Collieran, H. L., Ibrahim, S. A., & da Silva, R. C. (2022). Potential Use of Carnauba Wax Oleogel to Replace Saturated Fat in Ice Cream. *Journal of the American Oil Chemists' Society*, 99(11), 1085–1099. <https://doi.org/10.1002/aocs.12652>
- Blake, A. I., Co, E. D., & Marangoni, A. G. (2014). Structure and physical properties of plant wax crystal networks and their relationship to oil binding capacity. *Journal of the American Oil Chemists' Society*, 91(6), 885–903. <https://doi.org/10.1007/s11746-014-2435-0>
- Blake, A. I., & Marangoni, A. G. (2015). The Use of Cooling Rate to Engineer the Microstructure and Oil Binding Capacity of Wax Crystal Networks. *Food Biophysics*, 10, 456–465. <https://doi.org/10.1007/s11483-015-9409-0>
- Chen, F., Zhang, H., Sun, X., Wang, X., & Xu, X. (2013). Effects of ultrasonic parameters on the crystallization behavior of palm oil. *Journal of the American Oil Chemists' Society*, 90(7), 941–949. <https://doi.org/10.1007/s11746-013-2243-y>
- Co, E. D., & Marangoni, A. G. (2012). Organogels: An alternative edible oil-structuring method. *Journal of the American Oil Chemists' Society*, 89, 749–780. <https://doi.org/10.1007/s11746-012-2049-3>
- Daniel, J., & Rajasekharan, R. (2003). Organogelation of plant oils and hydrocarbons by long-chain saturated FA, fatty alcohols, wax esters, and dicarboxylic acids. *JAOCS, Journal of the American Oil Chemists' Society*, 80(5), 417–421. <https://doi.org/10.1007/s11746-003-0714-0>
- Dassanayake, L. S. K., Kodali, D. R., Ueno, S., & Sato, K. (2009). Physical properties of rice bran wax in bulk and organogels. *JAOCS, Journal of the American Oil Chemists' Society*, 86(12), 1163–1173. <https://doi.org/10.1007/s11746-009-1464-6>
- Doan, C. D., Davy, V. D. W., Patel, A. R., & Dewettinck, K. (2015). Evaluating the Oil-Gelling Properties of Natural Waxes in Rice Bran Oil: Rheological, Thermal, and Microstructural Study. *Journal of the American Oil Chemists' Society*, 92, 801–811. <https://doi.org/10.1007/s11746-015-2645-0>
- Doan, C. D., Tavernier, I., Sintang, M. D., Bin Dhanthine, S., Van de Walle, D., Rimaux, T., & Dewettinck, K. (2017). Crystallization and Gelation Behavior of Low- and High Melting Waxes in Rice Bran Oil: a Case-Study on Berry Wax and Sunflower Wax. *Food Biophysics*, 12(1), 97–108. <https://doi.org/10.1007/s11483-016-9467-y>
- Doan, C. D., To, C. M., De Vrieze, M., Lynen, F., Dhanthine, S., Brown, A., ... Patel, A. R. (2017). Chemical profiling of the major components in natural waxes to elucidate their role in liquid oil structuring. *Food Chemistry*, 214, 717–725. <https://doi.org/10.1016/j.foodchem.2016.07.123>
- Giacomozi, A., Palla, C., Carrin, M. E., & Martini, S. (2020). Tailoring physical properties of monoglycerides oleogels using high-intensity ultrasound. *Food Research International*, 134(April), 109,231. <https://doi.org/10.1016/j.foodres.2020.109231>
- Giacomozi, A. S., Palla, C. A., Carr, E., & Martini, S. (2019). Physical Properties of Monoglycerides Oleogels Modified by Concentration, Cooling Rate, and High-Intensity Ultrasound. *Journal of Food Science*, 84(9), 2549–2561. <https://doi.org/10.1111/1750-3841.14762>
- Guillen, M. D., & Cabo, N. (1997). Infrared Spectroscopy in the Study of Edible Oils and Fats. *Journal of Science and Food Agriculture*, 75, 1–11. [https://doi.org/10.1002/\(SICI\)1097-0010\(199709\)75:1 <1::AID-JSFA842 >3.0.CO;2-R](https://doi.org/10.1002/(SICI)1097-0010(199709)75:1 <1::AID-JSFA842 >3.0.CO;2-R)
- Hwang, H.-S., Sanghoon, K., Singh, M., Winkler-Moser, J. K., Kim, S., & Liu, S. X. (2012). Organogel Formation of Soybean Oil with Waxes. *Journal of the American Oil Chemists' Society*, 89, 639–647. <https://doi.org/10.1007/s11746-011-1953-2>
- Hwang, H. S., Singh, M., Bakota, E. L., Winkler-Moser, J. K., Kim, S., & Liu, S. X. (2013). Margarine from organogels of plant wax and soybean oil. *Journal of the American Oil Chemists' Society*, 90(11), 1705–1712. <https://doi.org/10.1007/s11746-013-2315-z>
- Jadhav, H. B., Pratap, A. P., Gogate, P. R., & Annapure, U. S. (2022). Ultrasound-assisted synthesis of highly stable MCT based oleogel and evaluation of its baking performance. *Applied Food Research*, 2(2), 100,156. <https://doi.org/10.1016/j.afres.2022.100156>
- Jana, S., & Martini, S. (2014). Effect of high-intensity ultrasound and cooling rate on the crystallization behavior of beeswax in edible oils. *Journal of Agricultural and Food Chemistry*, 62(41), 10192–10202. <https://doi.org/10.1021/jf503393h>
- Leighton, T. G. (1994). *The acoustic bubble*. Academic Press.
- Li, L., Taha, A., Geng, M., Zhang, Z., Su, H., Xu, X., Pan, S., & Hu, H. (2021). Ultrasound-assisted gelation of  $\beta$ -carotene enriched oleogels based on candelilla wax-nut oils: Physical properties and *in-vitro* digestion analysis. *Ultrasonics Sonochemistry*, 79 (105), 762. <https://doi.org/10.1016/j.ulsonch.2021.105762>
- Martini, S., Suzuki, A. H., & Hartel, R. W. (2008). Effect of high intensity ultrasound on crystallization behavior of anhydrous milk fat. *Journal of the American Oil Chemists' Society*, 85(7), 621–628. <https://doi.org/10.1007/s11746-008-1247-5>
- Martini, S., Tan, C. Y., & Jana, S. (2015). Physical Characterization of Wax/Oil Crystalline Networks. *Journal of Food Science*, 80(5), C989–C997. <https://doi.org/10.1111/1750-3841.12853>
- Mattice, K. D., & Marangoni, A. G. (2018). Fat Crystallization and Structure in Bakery, Meat, and Cheese Systems. In A. G. Marangoni (Ed.), *Structure-Function Analysis of Edible Fats* (Second, pp. 287–311). AOCS press. Doi:10.1016/B978-0-12-814041-3.00010-1.
- Menard, K. P., & Menard, N. R. (2020). Dynamic mechanical analysis. In K. P. Menard, & N. R. Menard (Eds.), *ThirdVol. 31, Issue 1. American Chemical Society, Polymer Preprints, Division of Polymer Chemistry*. CRC Press: Taylor & Francis Group. <https://doi.org/10.3139/9781569906446.012>
- Okuro, P. K., Tavernier, I., Sintang, D. B., Skirtach, A. G., Vicente, A. A., Dewettinck, K., & Cunha, R. L. (2018). Synergistic interactions between lecithin and fruit wax in oleogel formation. *Food & Function*, 9, 1755–1767. <https://doi.org/10.1039/c7fo01775h>
- Patel, A. R., Babaahmadi, M., Lesaffer, A., & Dewettinck, K. (2015). Rheological Profiling of Organogels Prepared at Critical Gelling Concentrations of Natural Waxes in a Triacylglycerol Solvent. *Journal of Agricultural and Food Chemistry*, 63(19), 4862–4869. <https://doi.org/10.1021/acs.jafc.5b01548>
- Patel, A. R., & Dewettinck, K. (2015). Comparative evaluation of structured oil systems: Shellac oleogel, HPMC oleogel, and HIPE gel. *European Journal of Lipid Science and Technology*, 117(11), 1772–1781. <https://doi.org/10.1002/ejlt.201400553>
- Patel, A. R., Schatteman, D., De Vos, W. H., Lesaffer, A., & Dewettinck, K. (2013). Preparation and rheological characterization of shellac oleogels and oleogel-based emulsions. *Journal of Colloid and Interface Science*, 411, 114–121. <https://doi.org/10.1016/j.jcis.2013.08.039>
- Penagos, I. A., Murillo Moreno, J. S., Dewettinck, K., & Van Bockstaele, F. (2023). Carnauba Wax and Beeswax as Structuring Agents for Water-in-Oleogel Emulsions without Added Emulsifiers. *Foods*, 12(9). <https://doi.org/10.3390/foods12091850>
- Podmaniczky, F., & Gránásky, L. (2022). Molecular scale hydrodynamic theory of crystal nucleation and polycrystalline growth. *Journal of Crystal Growth*, 597(June). <https://doi.org/10.1016/j.jcrysgro.2022.126854>
- Rocha, J. C. B., Lopes, J. D., Mascarenhas, M. C. N., Arellano, D. B., Guerreiro, L. M. R., & da Cunha, R. L. (2013). Thermal and rheological properties of organogels formed by sugarcane or candelilla wax in soybean oil. *Food Research International*, 50(1), 318–323. <https://doi.org/10.1016/j.foodres.2012.10.043>
- Rumayor-Escobar, A., de la Peña, M. M., de la Rosa-Millán, J., Arredondo-Ochoa, T., Dibildox-Alvarado, E., & Tejada-Ortizgo, V. (2023). Effect of high intensity ultrasound on soybean and avocado oleogels' structure and stability. *Food Structure*, 36(100), 315. <https://doi.org/10.1016/j.foosr.2023.100315>
- Sejwar, H., Singh, A., Kumar, N., Srivastava, S., Upadhyay, A., & Dar, A. H. (2024). Effect of ultrasonication on the properties of carnauba wax-based soybean oleogel. *Applied Acoustics*, 216(June 2023). <https://doi.org/10.1016/j.apacoust.2023.109729>

- Sharifi, M., Goli, S. A. H., & Fayaz, G. (2019). Exploitation of high-intensity ultrasound to modify the structure of olive oil organogel containing propolis wax. *International Journal of Food Science and Technology*, 54, 509–515. <https://doi.org/10.1111/ijfs.13965>
- Shi, Y., Liu, C., Zheng, Z., Chai, X., Han, W., & Liu, Y. (2021). Gelation behavior and crystal network of natural waxes and corresponding binary blends in high-oleic sunflower oil. *Journal of Food Science*, 86(9), 3987–4000. <https://doi.org/10.1111/1750-3841.15840>
- da Silva, T. L. T., Arellano, D. B., & Martini, S. (2019). Interactions between candelilla wax and saturated triacylglycerols in oleogels. *Food Research International*, 121, 900–909. <https://doi.org/10.1016/j.foodres.2019.01.018>
- da Silva, T. L. T., Baeten, V., & Danthine, S. (2023). Modifying sucrose esters oleogels properties using different structuration routes. *Food Chemistry*, 405(PB), 134927. <https://doi.org/10.1016/j.foodchem.2022.134927>
- da Silva, T. L. T., Chaves, K. F., Fernandes, G. D., Rodrigues, J. B., Bolini, H. M. A., & Arellano, D. B. (2018). Sensory and Technological Evaluation of Margarines With Reduced Saturated Fatty Acid Contents Using Oleogel Technology. *Journal of American Oil Chemistry Society*, 95(6), 673–685. <https://doi.org/10.1002/aocs.12074>
- da Silva, T. L. T., Cooper, Z., Lee, J., Gibon, V., & Martini, S. (2020). Tailoring Crystalline Structure Using High-Intensity Ultrasound to Reduce Oil Migration in a Low Saturated Fat. *Journal of the American Oil Chemists' Society*, 97, 141–155. <https://doi.org/10.1002/aocs.12321>
- da Silva, T. L. T., & Danthine, S. (2021). Effect of high-intensity ultrasound on the oleogelation and physical properties of high melting point monoglycerides and triglycerides oleogels. *Journal of Food Science*, 86(2), 343–356. <https://doi.org/10.1111/1750-3841.15589>
- da Silva, T. L. T., Fernandes, G. D., & Arellano, D. B. (2021). Development of reduced saturated fat cookie fillings using multicomponent oleogels. *Journal of the American Oil Chemists' Society*, 48(11), 1069–1082. <https://doi.org/10.1002/aocs.12527>
- da Silva, T. L. T., Fernandes, G. D., & Arellano, D. B. (2022). The combination of monoglycerides, wax and hardfat on oleogels structuration. *Brazilian Journal of Food Technology*, 25, 1–16. <https://doi.org/10.1590/1981-6723.13721>
- Suzuki, A. H., Lee, J., Padilla, S. G., & Martini, S. (2010). Altering Functional Properties of Fats Using Power Ultrasound. *Food Engineering and Physical Properties*, 75(4), 208–214. <https://doi.org/10.1111/j.1750-3841.2010.01572.x>
- Tavernier, I., Doan, C. D., Van der Meer, P., Heyman, B., & Dewettinck, K. (2018). The Potential of Waxes to Alter the Microstructural Properties of Emulsion-Templated Oleogels. *European Journal of Lipid Science and Technology*, 120(3), 1–13. <https://doi.org/10.1002/ejlt.201700393>
- Teodoro da Silva, T. L., & Danthine, S. (2022). Influence of sonocrystallization on lipid crystals multicomponent oleogels structuration and physical properties. *Food Research International*, 154(110), 997. <https://doi.org/10.1016/j.foodres.2022.110997>
- Toro-Vazquez, J. F., Morales-Rueda, J. A., Dibildox-Alvarado, E., Charó-Alonso, M., Alonzo-Macias, M., & González-Chávez, M. M. (2007). Thermal and textural properties of organogels developed by candelilla wax in safflower oil. *JAACS, Journal of the American Oil Chemists' Society*, 84(11), 989–1000. <https://doi.org/10.1007/s11746-007-1139-0>
- Trappe, V., & Weitz, D. A. (2000). Scaling of the viscoelasticity of weakly attractive particles. *Physical Review Letters*, 85(2), 449–452. <https://doi.org/10.1103/PhysRevLett.85.449>
- Ueno, S., Ristic, R. I., Higaki, K., & Sato, K. (2003). *In Situ* Studies of Ultrasound-Stimulated Fat Crystallization Using Synchrotron Radiation. *The Journal of Physical Chemistry B*, 107(21), 4927–4935. <https://doi.org/10.1021/jp027840f>
- Ye, Y., & Martini, S. (2015). Application of high-intensity ultrasound to palm oil in a continuous system. *Journal of Agricultural and Food Chemistry*, 63(1), 319–327. <https://doi.org/10.1021/jf505041s>
- Ye, Y., Wagh, A., & Martini, S. (2011). Using high intensity ultrasound as a tool to change the functional properties of interesterified soybean oil. *Journal of Agricultural and Food Chemistry*, 59(19), 10712–10722. <https://doi.org/10.1021/jf202495b>
- Yilmaz, E., Keskin Uslu, E., & Öz, C. (2021). Oleogels of Some Plant Waxes: Characterization and Comparison with Sunflower Wax Oleogel. *Journal of the American Oil Chemists' Society*, 98, 643–655. <https://doi.org/10.1002/aocs.12490>